Communications

Dual-Band Multiple Beam Antenna System Using Hybrid-Cell Reuse Scheme for Non-Uniform Satellite Communications Traffic

Jim Wang, Sudhakar K. Rao, Minh Tang, and Chih-Chien Hsu

***Abstract*—An advanced dual-band antenna system suitable for broadband satellites that is capable of providing higher EIRP, higher G/T, and improved copolar isolation among frequency reuse beams is presented. The antenna system employs a hybrid-cell frequency reuse scheme instead of conventional fixed cell reuse (4-cell or 7-cell) in order to efficiently use spectrum based on traffic demands. It is shown that the advanced antenna employing high-efficiency horns and shaped reflectors provides about 1.0 dB EIRP improvement, 2.0 dB G/T improvement, and 3.0 dB improvement in C/I when compared to conventional antennas.**

***Index Terms*—Dual-band horns, high efficiency horns, reflector antennas, satellite antennas.**

I. Introduction

There has been a significant growth in the broadband communications satellite market in the recent past. These systems provide communications among several users that are spread over a given coverage region by using multiple overlapping spot beams. Communications among users is established through the hubs and the satellite. The users within the coverage region establish two-way communications links with other users via the satellites and the hubs through forward (hub uplink and user downlink) and return (user uplink and hub downlink) links. This requires that each spot beam on-board the satellite needs to support simultaneously Ka-band uplink signals and K-band downlink signals that are spread over large bandwidth ratio of about 1.64. This communication discusses advanced dual-band antenna system employing dual-band high efficiency horns (DBHEH) [1], shaped reflectors, and use of hybrid-cell reuse scheme [2] that provides significant improvements in RF performance and efficient traffic distribution within the coverage region.

II. Hybrid-Cell Reuse Scheme

Fig. 1 shows typical layout of the multiple beam antenna (MBA) in the deployed view of the spacecraft. It employs four multiple reflector apertures, where by each reflector is fed with multiple horns producing about one fourth of the total number of spot beams. The beams from the four reflectors are interleaved on ground with hexagonal grid layout and providing contiguous spot beam coverage from a given orbital location of the satellite.

Conventional layout of the beams using a 4-cell fixed reuse scheme is shown in Fig. 2. There are 45 spot beams covering CONUS from 105 W orbital slot, each with a diameter of 0.7° and with adjacent beam spacing of 0.6°. RF performance of each beam needs to be evaluated by expanding the beam diameter including satellite pointing error. Alternate beams are generated from the same reflector. A total of 16 channels are used with each beam carrying four channels on the four-cell re-use pattern using cells A, B, C, & D. The disadvantage with this approach is that each beam has the identical capacity independent of the population density and demand, carries a total of 180 channels that are too many to support for any spacecraft, and requires a large number (12 for this example) of hubs on the ground.

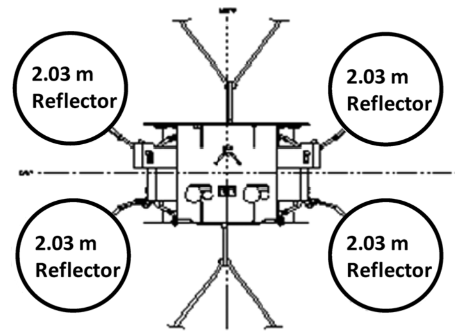

Fig. 1. Typical MBA spacecraft layout.

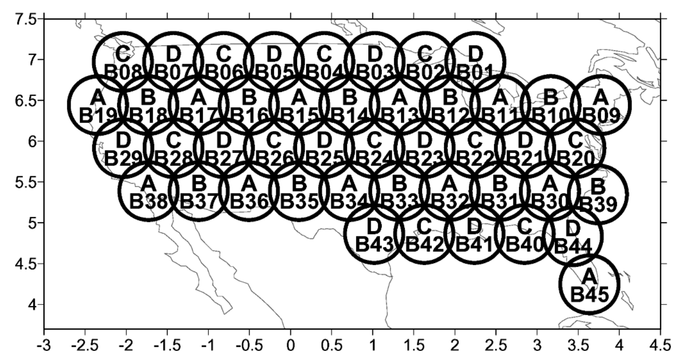

Fig. 2. Conventional MBA using 4-Cell reuse.

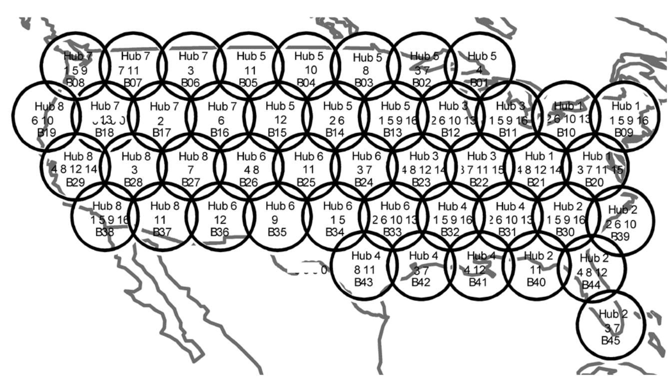

Fig. 3. MBA using proposed "hybrid-cell" reuse.

The hybrid-cell reuse scheme, shown in Fig. 3, overcomes most of above limitations of the fixed-cell reuse scheme. Each beam has designations of the beam number, hub number, and specific channel numbers it is using out of the 16 available channels (8 channels are left-hand

Manuscript received June 25, 2009; revised July 31, 2009; accepted October 02, 2009. Date of publication January 26, 2010; date of current version April 07, 2010.

The authors are with Lockheed Martin Space Systems Company, Newtown, PA 18966 USA (e-mail: jim.wang@lmco.com; sudhakar.rao@lmco.com; minh.tang@lmco.com; chih-chien.hsu@lmco.com).

Color versions of one or more of the figures in this communication are available online at http://ieeexplore.ieee.org.

Digital Object Identifier 10.1109/TAP.2010.2041172

circularly polarized and the remaining 8 channels are right-hand circularly polarized). It employs a 4-cell reuse scheme for the densely populated areas such as east-coast and west-coast and an N-cell reuse scheme $(N > 4)$ for the low population regions of the contiguous US (CONUS). All the east-coast and west-coast beams with high population density carry 4 channels each, while the beams located in the mid-west, north, and south-west of CONUS with low population density carry 1 to 3 channels each depending on the population and traffic demand in these beams. This method provides capacity in each beam based on the traffic demand, requires only 107 total number of channels that can be supported by several spacecrafts in the industry, and demands only 8 hubs to support both forward and return channels. The hybrid-cell reuse scheme provides tremendous flexibility in the beam/channel layout, and provides better overall antenna carrier-to-interference ratio (C/I) for the beams. The C/I is the aggregate value where all the copolar and cross-polar interferers are added in power and compared to the carrier within the beam.

III. Dual-Band Antenna

The MBA shown in Fig. 1 employs four graphite reflectors, each being fed with about 12 horns to generate about 12 beams. The antenna has to support downlink beams at K-band (20 GHz) and uplink beams at Ka-band (30 GHz). Conventional antennas are designed with reflector size meeting the desired beam size at the downlink K-band. However, the uplink beams at Ka-band are 50% smaller than the downlink beams due to larger electrical size of the reflector and suffer from lower edge-of-coverage (EOC) gain, increased gain loss due to pointing error, and suffer from large peak-to-edge gain variation and lower C/I.

Advanced MBA design for the dual-band antenna employs the following design features to achieve significant performance advantages at both bands.

- High-efficiency dual-band horns [1], [3] with more than 82% efficiency at both bands (conventional corrugated horn has about 54% efficiency) to provide more illumination taper on the reflector resulting in improved EOC gain and lower sidelobes that improve C/I on the downlink;
- Shaped reflector surface to broaden the receive beams to improve EOC gain, reduce peak-to-edge variation, and improve C/I on the uplink beams. The shaping will have minimal impact on downlink beams EOC gain;
- Stepped-reflector to generate a flat-top receive beam and improve G/T performance;
- Use of hybrid-cell reuse scheme to provide non-uniform traffic based on the population density, to reduce the number of required hubs, and to improve C/I.

The high efficiency horn (HEH) employs TE1m type modes (TE12, TE13, TE14, TE15 etc.) in addition to the dominant TE11 mode to make the aperture illumination more uniform resulting in higher efficiency. The DBHEH typical geometry is shown in Fig. 4 and it employs five "slope-discontinuities" to generate the desired higher order modes in order to achieve high efficiency of $>82\%$ at both bands. The horn geometry is synthesized using the mode-matching analysis of discrete step-junctions combined with a generalized scattering matrix (GSM) to evaluate the horn performance. Fig. 5 shows performance of DBHEH compared to other conventional horns, such as corrugated and Potter type horns. Note that the Potter horn model is ideal and can not be realized in practice due to its bandwidth limitations. These primary patterns are used to evaluate the secondary patterns of an 80 in. offset reflector antenna. The reflector surface is shaped mainly to broaden the receive beams and thereby improving the radiation patterns at Rx frequencies. The edge of coverage gain and worst case C/I of the antenna beams are evaluated by enlarging the beam size to account for the satellite pointing error of $+/-0.05^\circ$ i.e., using 0.8° beam instead of the nominal 0.7° beam. The carrier-to-interference ratio (C/I) is calculated in an aggregate manner that includes power addition of all the copolar interferers coming from several adjacent beams that re-use the same frequency as the carrier and also cross-polar interferences. Table I summarizes performance comparison of the MBA with DBHEH and conventional corrugated horn. The DBHEH improves the EOC gain by about 0.9 dB at Tx and by about 2.0 dB at Rx, and improves the Tx C/I by about 3.0 dB.

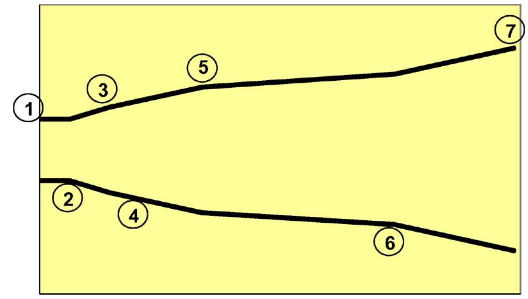

Fig. 4. Typical geometry of DBHEH using "slope-discontinuities".

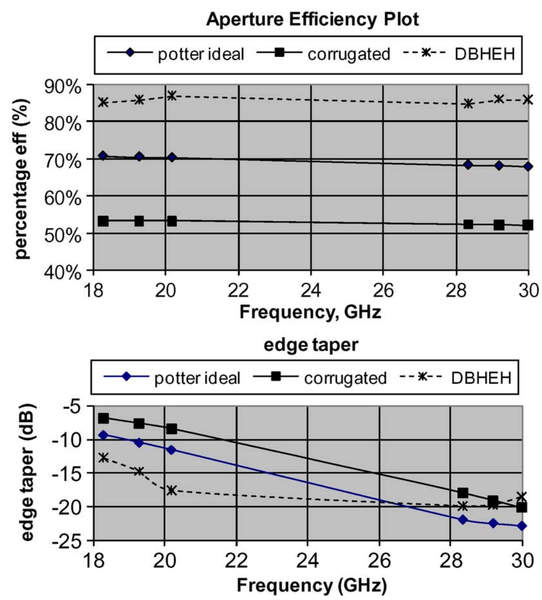

Fig. 5. Aperture efficiency and edge taper comparison of various dual-band MBA horns.

TABLE I
RF Performance Comparison of Primary and Secondary Patterns of the DBHEH With Conventional Corrugated Horn

Performance Parameter	CONVENTIONAL HORN (CORRUGATED)	DBHEH
	TX/RX	TX/RX
Efficiency, %	**54 / 52**	**85 / 85**
Edge Taper, dB	7/18	13 / 17
Primary C/X, dB	33 / 33	20 / 23
EOC Directivity, dBi	**43.8 / 41.7**	**44.7 / 43.7**
C/I, 3-cell(dB)	11.1 / 13.0	14.2 / 11.6
C/I, 4-cell(dB)	12.0 / 15.8	15.7 / 14.5
C/I, 7-cell (dB)	**18.2 / 19.5**	**22.7 / 21.9**
C/X, dB	30.0 / 28.0	21.0 / 20.0

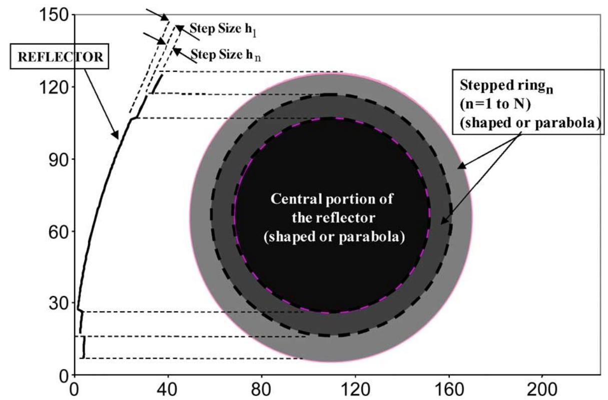

Fig. 6. Concept of "Stepped Reflector Antenna".

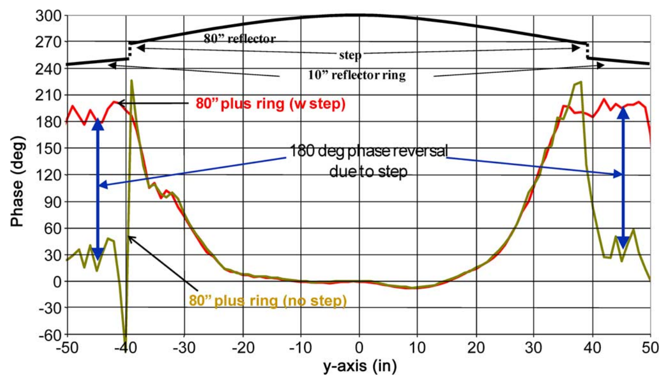

Fig. 7. Near-field phase distribution of the SRA at Rx frequencies.

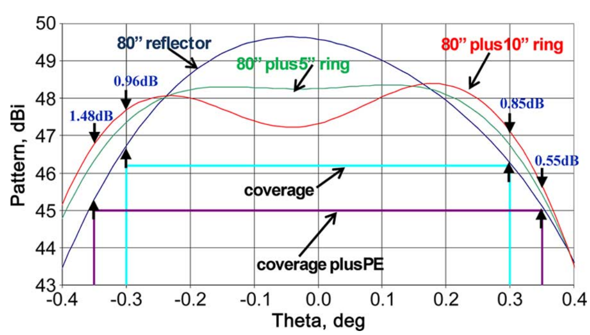

Fig. 8. Computed DMBA patterns of the SRA showing "flat-topped" beam with increased EOC gain.

The DMBA performance can be further improved by the use of Lockheed Martin's patented "stepped-reflector antenna" (SRA) technology [4]. The SRA concept is illustrated in Fig. 6 where it employs an outer annular region that is stepped relative to the central region. The height of the stepped region is designed in conjunction with the DBHEH feed phase characteristics at the Rx frequencies in order to provide a 180 degree phase reversal in the stepped region resulting in a "flat-topped" receive beam with improved EOC gain. Both central and outer annular regions can be shaped to improve the overall RF performance and the transition region can be blended smoothly near the stepped region to avoid abrupt discontinuities.

The computed near-field phase patterns of the SRA plotted in Fig. 7 show the 180-degree phase reversal at Rx frequencies near the transition region of the step. As a result, the Rx beam patterns computed in Fig. 8 show "flat-topped" radiation patterns with increased

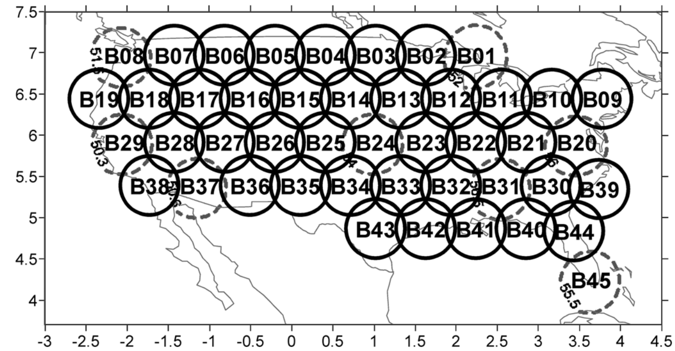

Fig. 9. Computed EIRP contours of MBA.

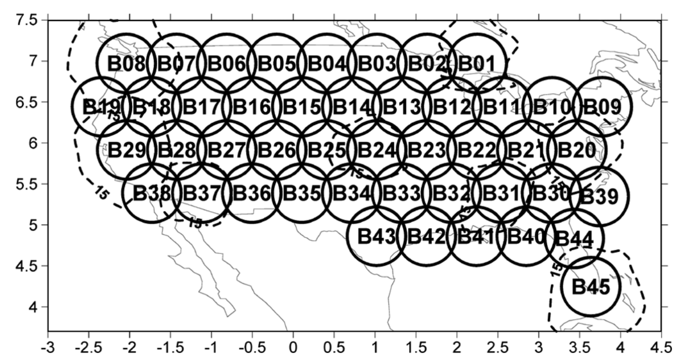

Fig. 10. Computed C/I contours of Tx MBA.

EOC gain. EOC gain improvement at Rx band is about 1.2 dB relative to the conventional reflector. The feed horn will have a quadratic error across the reflector aperture due to the fact that it is typically aligned with the reflector such that the Tx phase center coincides with the focal-plane of the reflector. The Rx phase center will be away from the focal-plane and inside the horn which results in a quadratic phase front across the reflector aperture. This property could be utilized to reduce the step height from quarter wavelength to less than quarter length depending on the DBHEH design. The reduced step size eases the fabrication of the shaped reflector blending the smaller step smoothly into its surface.

By combining the fed quadratic phase variation and the phase variation due to the stepped region, the height of the step can be minimized allowing the stepped region to be blended with the reflector shape. The SRA concept works well for wide angle coverage regions like CONUS and achieves significant improvements in Rx gain, Rx C/I, Tx C/I, and moderate improvement of Tx gain when compared to a reflector without the step region. Typical computed EIRP and C/I patterns of the spot beams over the CONUS coverage are shown in Figs. 9 & 10, respectively. The EIRP is weighted to give higher values over the rain regions and the C/I values are better than 18 dB on the average. The coverage region is not shown in Fig. 9 for those beams with EIRP computations for better clarity.

IV. Summary and Conclusion

An advanced multiple beam antenna that provides communications traffic based on the population density and demand is presented. It employs a hybrid-cell frequency reuse scheme to provide non-uniform traffic distribution. By employing dual-band high efficiency horns, shaped reflectors, and stepped-reflector with annular region, it is shown that significant improvement of the order of 1.0 dB for EIRP, 3.0 dB for G/T, and 3.0 dB for C/I can be achieved over conventional

MBA designs. It is feasible to provide limited on-orbit reconfigurability for future satellites in terms of number of channels per beam by using switch matrices at the payload repeater level. The trades are the flexibility versus added complexity of the switch matrices and its associated losses.

Acknowledgment

The authors thank the anonymous reviewers for their valuable suggestions that have helped to improve the quality of the communication.

References

[1] S. Rao and M. Tang, "High-efficiency horns for an antenna system," U.S. Patent 7,463,207, Dec. 09, 2008, Lockheed Martin.

[2] S. Rao, M. Sheshadri, and J. Wang, "Multiple-beam antenna system using hybrid frequency-reuse scheme," U.S. Patent 7,382,743, Jun. 03, 2008, Lockheed Martin.

[3] S. Rao, K. K. Chan, and M. Tang, "Design of high efficiency circular horn feeds for multibeam reflector applications," in *Proc. IEEE AP-S Symp.*, Washington, DC, Jul. 2005, pp. 359–362.

[4] S. Rao and M. Tang, "Stepped-reflector antenna for dual-band multiple beam satellite communications payloads," *IEEE Trans. Antennas Propag.*, vol. 54, pp. 801–811, Mar. 2006.

A Low Cross-Polarization Smooth-Walled Horn With Improved Bandwidth

Lingzhen Zeng, Charles L. Bennett, David T. Chuss, and Edward J. Wollack

***Abstract*—Corrugated feed horns offer excellent beam symmetry, main beam efficiency, and cross-polar response over wide bandwidths, but can be challenging to fabricate. An easier-to-manufacture smooth-walled feed is explored that approximates these properties over a finite bandwidth. The design, optimization and measurement of a monotonically-profiled, smooth-walled scalar feedhorn with a diffraction-limited $\sim 14^\circ$ FWHM beam is presented. The feed was demonstrated to have low cross polarization (< -30 dB) across the frequency range 33–45 GHz (30% fractional bandwidth). A power reflection below -28 dB was measured across the band.**

***Index Terms*—Feeds, horn antennas, millimeter-wave antennas.**

I. Introduction

Many precision microwave applications, including those associated with radio astronomy, require feedhorns with symmetric E- and H-plane beam patterns that possess low sidelobes and cross-polarization control. A common approach to achieving these goals is a "scalar" feed, which has a beam response that is independent of azimuthal angle. Corrugated feeds [1] approximate this idealization by providing the appropriate boundary conditions for the HE_{11} hybrid mode at the feed aperture. Alternatively, an approximation to a scalar feed can be obtained with a multimode feed design. One such "dual-mode" horn is the Potter horn [2]. In this implementation, an appropriate admixture of TM_{11} is generated from the initial TE_{11} mode using a concentric step discontinuity in the waveguide. The two modes are then phased to achieve the proper field distribution at the feed aperture using a length of waveguide. The length of the phasing section limits the bandwidth due to the dispersion between the modes. Lier [3] has reviewed the cross-polarization properties of dual-mode horn antennas for selected geometries. Other authors have produced variations on this basic design concept [4], [5]. Improvements in the bandwidth have been realized by decreasing the phase difference between the two modes by 2π [6], [7].

To increase the bandwidth, it is possible to add multiple concentric step continuities with the appropriate modal phasing [8], [9]. A variation on this technique is to use several distinct linear tapers to generate the proper modal content and phasing [10], [11]. Operational bandwidths of 15–20% have been reported using such techniques. A related class of devices is realized by allowing the feedhorn profile to vary smoothly rather than in discrete steps. Examples of such smooth-walled feedhorns with $\sim$15% fractional bandwidths exist in the literature [12], [13].

In this work, we describe the design and optimization of a smooth-walled feed that has a 30% operational bandwidth, over which the cross-polarization response is better than -30 dB. The optimization technique is described, and the performance of the feed is compared with other published dual-mode feedhorns. The feedhorn described here has a monotonic profile that allows it to be manufactured by progressively milling the profile using a set of custom tools.

Manuscript received July 10, 2009; revised October 16, 2009; accepted November 08, 2009. Date of publication January 26, 2010. Date of current version April 07, 2010. This work was supported in part by a NASA ROSES APRA Grant and a Johns Hopkins University/APL partnership research grant.

L. Zeng and C. L. Bennett are with the Department of Physics and Astronomy, The Johns Hopkins University, Baltimore, MD 20723 USA (e-mail: lingzz@pha.jhu.edu; cbennett@pha.jhu.edu).

D. T. Chuss and E. J. Wollack are with the Observational Cosmology Laboratory, NASA GSFC, Greenbelt, MD 20771 USA (e-mail: David.T.Chuss@nasa.gov; Edward.J.Wollack@nasa.gov).

Digital Object Identifier 10.1109/TAP.2010.2041318

II. Smooth-Walled Feedhorn Optimization

The performance of a feedhorn can be characterized by angle- and frequency-dependent quantities that include beam width, sidelobe response and cross-polarization. Quantities such as reflection coefficient and polarization isolation that only depend on frequency are also important considerations. All of these functions are dependent upon the shape of the feed profile. In the optimization approach described, a weighted penalty function is used to explore and optimize the relationship between the feed profile and the electromagnetic response.

A. Beam Response Calculation

The smooth-walled horn was approximated by a profile that consists of discrete waveguide sections, each of constant radius. With this approach, it was important to verify that each section is thin enough that the model is a valid approximation of the continuous profile. For profiles relevant to our design parameters, section lengths of $\Delta l \leq \lambda_c/20$ were found to be sufficient by trial and error, where λ_c is the cutoff wavelength of the input waveguide section. It is possible in principle to dynamically set the length of each section to optimize the approximation to the local curvature of the horn. This would increase the speed of the optimization; however, for simplicity, this detail was not implemented in our study.

For each trial feedhorn the angular response was calculated directly from the modal content at the feed aperture. This in turn was calculated as follows. The throat of the feedhorn was assumed to be excited by the circular waveguide TE_{11} mode. The modal content of each successive section was then determined by matching the boundary conditions at each interface using the method of James